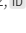


[Re] A circuit model of auditory cortexParvathy Neelakandan¹ and Christoph Metzner^{1,2, }¹Neural Information Processing Group, Institute of Software Engineering and Theoretical Computer Science, Technische Universität Berlin, Berlin, Germany – ²Biocomputation Group, Centre for Computer Science and Informatics Research, University of Hertfordshire, Hatfield, United KingdomEdited by
(Editor)Received
–Published
–DOI
–**Introduction**

bla

Methods

In this replication, we focus on the rate models proposed in the original article. The firing rate model was an extensions of the traditional Wilson-Cowan model¹ and represented an iso-frequency unit of the auditory cortex. This iso-frequency unit consisted of one excitatory and two inhibitory populations. Building on this unit a more complex three-unit rate models was developed, to investigate stimulus-specific adaptation, forward suppression, tunig-curve adaptation and feedforward functional connectivity.

Iso-Frequency Unit Model The iso-frequency unit model was based on the Wilson-Cowan model¹ but was modified to include two different types of inihbitory interneurons. The two inhibitory population are meant to represent parvalbumin-psoitve (PV) and somatostatin (SST) cells. The single unit model is given by

$$\tau_u \frac{du(t)}{dt} = -u(t) + f(w_{ee}u(t) - w_{ep}p(t) - w_{es}s(t) + qg(t)i(t)), \quad (1)$$

$$\tau_p \frac{dp(t)}{dt} = -p(t) + f(w_{pe}u(t) - w_{pp}p(t) - w_{ps}s(t) + I_{Opt,PV}(t) + qg(t)i(t)), \quad (2)$$

$$\tau_s \frac{ds(t)}{dt} = -s(t) + f(w_{se}u(t) - w_{sp}p(t) - w_{ss}s(t) + I_{Opt,SST}(t)), \quad (3)$$

with $u(t)$, $p(t)$, and $s(t)$ being the normalized firing rates (in $[0, 1]$) of the pyramidal cell population, the PV population and the SST population, respectively. Furthermore, w_{xy} represents the strengths of connections from population y to population x . The two terms $I_{Opt,PV}$ and $I_{Opt,SST}$ describe the input current to cells due to optogenetic stimulation of the PV population and SST population, respectively. τ_i , $i \in u, p, s$ defines the time constants for the respective populaitons. The function f is realised as a threshold linear function given by

$$f(x) = \begin{cases} 0 & \text{if } x \leq 0 \\ rx & \text{if } 0 < x \leq 1/r \\ 1 & \text{if } x > 1/r, \end{cases}$$

Copyright © 2020 P. Neelakandan and C. Metzner, released under a Creative Commons Attribution 4.0 International license.
Correspondence should be addressed to Christoph Metzner (cmetzner@ni.tu-berlin.de)
The authors have declared that no competing interests exists.
Code is available at <https://github.com/ChristophMetzner/Park-Geffen-Replication>.

Table 1. Overview of the model parameters

a	b	c
1	2	3

(4)

which coarsely approximates a sigmoid function. Furthermore, the function f is thresholded by simply subtracting a constant u_i from the input x (i.e. $f(x - u_i)$) which varied for the different populations. Lastly, afferent auditory input is fed into the unit is given by $qg(t)i(t)$, which is subdivided into the 'raw' input $i(t)$ and a slow modulation $g(t)$ mimicking synaptic depression at thalamic synapses. The input function $i(t)$ is simply an instantaneous rise with amplitude q and an exponential decay with a time constant of τ_q . The synaptic depression $g(t)$ is governed by the following equation

$$\frac{dg(t)}{dt} = \frac{g_0 - g(t)}{\tau_{d1}} - \frac{g(t)i(t)}{\tau_{d2}}. \quad (5)$$

The parameter values can be found in Table 1

Three-Unit Model Building on the single unit a three-unit model was implemented, with each single unit representing a different input frequency, thus creating a simple tonotopic layout that allowed to explore more complex auditory inputs. Intra-unit connectivity was as described before for the single-unit model. Inter-unit connectivity was restricted to immediate neighbours and included the following connection types: Exc to exc, exc to PV and SST to exc. Together, the activity of the three populations of each unit was governed by

$$\tau_u \frac{du_i(t)}{dt} = -u_i(t) + f(w_{ee}u_i(t) - (w_{ep} - a(1 - D_i(t)))p_i(t) - w_{es}s_i(t) + J_{1,i}(t)), \quad (6)$$

$$\tau_p \frac{dp_i(t)}{dt} = -p_i(t) + f(w_{pe}u_i(t) - w_{pp}p_i(t) - w_{ps}s_i(t) + I_{Opt,PV}(t) + J_{2,i}(t)), \quad (7)$$

$$\tau_s \frac{ds_i(t)}{dt} = -s_i(t) + f(w_{se}u_i(t) - w_{sp}p_i(t) - w_{ss}s_i(t) + I_{Opt,SST}(t) + J_{3,i}(t)), \quad (8)$$

with

$$J_{1,i}(t) = \begin{cases} -F_i(t)s_2(t) + qI_i(t) + w_{ee}^*u_2(t) & \text{if } i = 1, 3 \\ -F_s(t)(s_1(t) + s_3(t)) + qI_2(t) + \frac{w_{ee}^*(u_1(t) + u_3(t))}{2} & \text{if } i = 2 \end{cases} \quad (9)$$

and

$$J_{2,i}(t) = \begin{cases} qI_i(t) + w_{pe}^*u_2(t) & \text{if } i = 1, 3 \\ qI_2(t) + \frac{w_{pe}^*(u_1(t) + u_3(t))}{2} & \text{if } i = 2 \end{cases} \quad (10)$$

and

$$J_{3,i}(t) = \begin{cases} qI_i(t) + w_{se}^*u_2(t) & \text{if } i = 1, 3 \\ qI_2(t) + \frac{w_{se}^*(u_1(t) + u_3(t))}{2} & \text{if } i = 2. \end{cases} \quad (11)$$

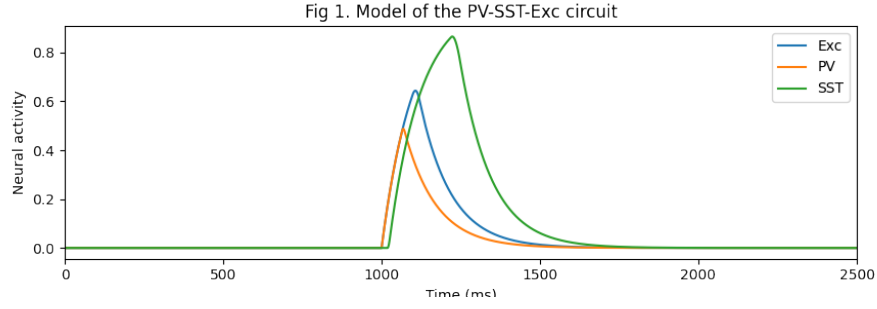


Figure 1. ReFig1

Here, $I_i(t)$ is described by

$$I_k(t) = g_k(t)i_k(t) + g_2(t)i_2(t)\alpha \quad \text{for } k = 1, 3 \quad (12)$$

and

$$I_2(t) = (g_1(t)i_1(t) + g_3(t)i_3(t))\alpha + g_2(t)i_2(t). \quad (13)$$

Here, $i_k(t)$ represents thalamic inputs to each of the three units. Taken together, the description of the three-unit model is the same than for the single-unit model, except for the addition of lateral inter-unit connectivity and short-term synaptic dynamics. Short-term facilitation is modelled by $F_i(t)$ and increases from 0 to positive values whereas depression is modelled by $D_i(t)$, which decreases from 1 towards 0. Facilitating synapses were added to Exc to SST inputs and depressing terms to PV to Exc synapses (see²). The facilitating term $F_j(t)$ obeys

$$\frac{dF_j(t)}{dt} = -\frac{F_j(t)}{\tau_{D_1}} + \frac{i_j(t)}{\tau_{D_2}}, \quad (14)$$

where τ_{D_1} and τ_{D_2} are again the depression time constants from the input functions of the single-unit model given in Equation 5. Analogously, the depression term $D_j(t)$ follows

$$\frac{dD_j(t)}{dt} = \frac{1 - D_j(t)}{\tau_{D_1}} - \frac{D_j(t)i_j(t)}{\tau_{D_2}}. \quad (15)$$

The choices for the parameters can again be found in Table 1 and were based on experimental studies^{3,4,5}.

Park and Geffen note that, when matching model behaviour to experimental findings, two distinct parameter sets emerged and a unified rate model description required a paradigm-dependent baseline inhibition, which reflected high thalamic activity (corresponding to weak baseline inhibition) versus low thalamic activity (corresponding to strong baseline inhibition). This was implemented using another variable \bar{F} governed by

$$\frac{d\bar{F}(t)}{dt} = \frac{\bar{F}^2(t)}{\tau_{F_1}} - \frac{\bar{I}(t)}{\tau_{F_2}}. \quad (16)$$

Reproduction of experiments

Reimplementation

The iso-frequency unit model and the three-unit model were both implemented in Python and integrated into the neurolib framework⁶.

Discussion

bla

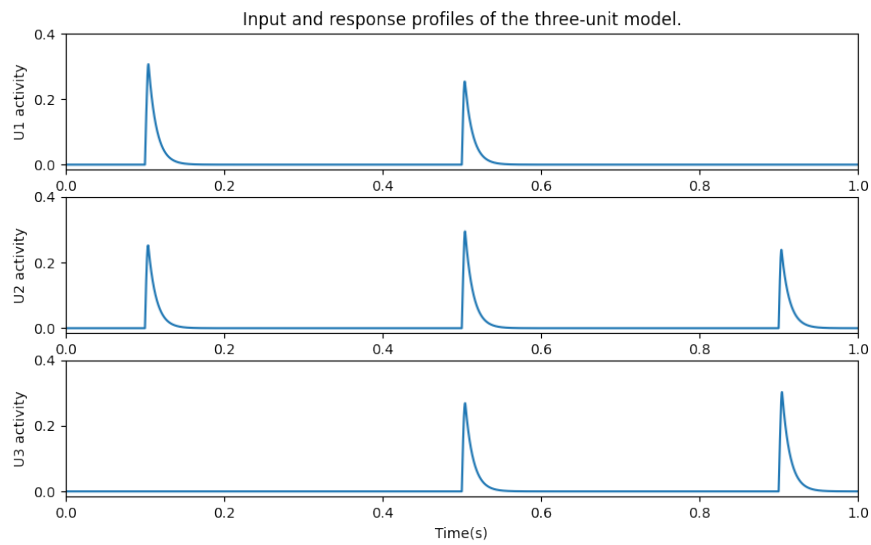


Figure 2. ReFig2

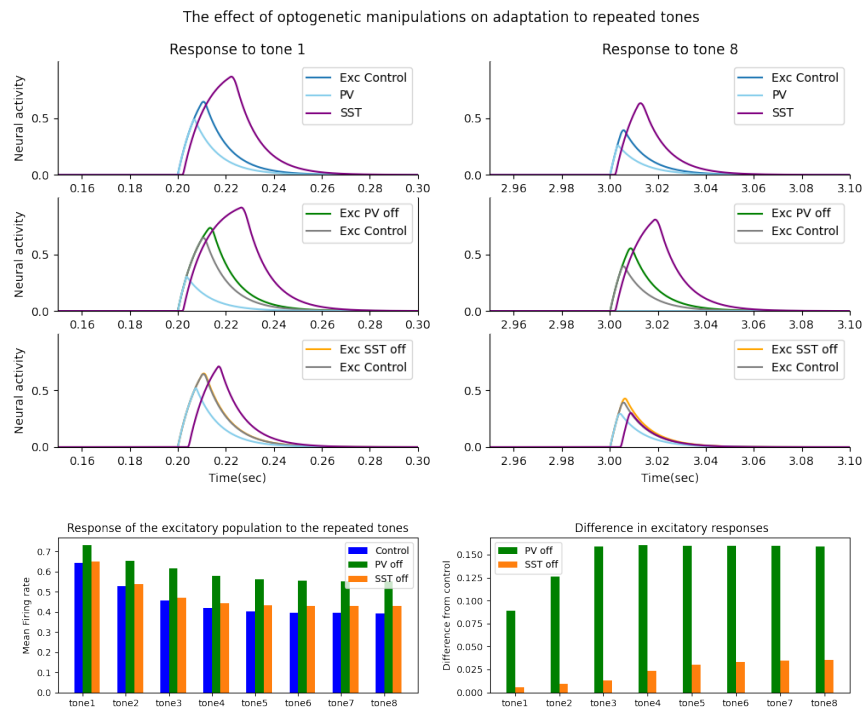


Figure 3. ReFig3

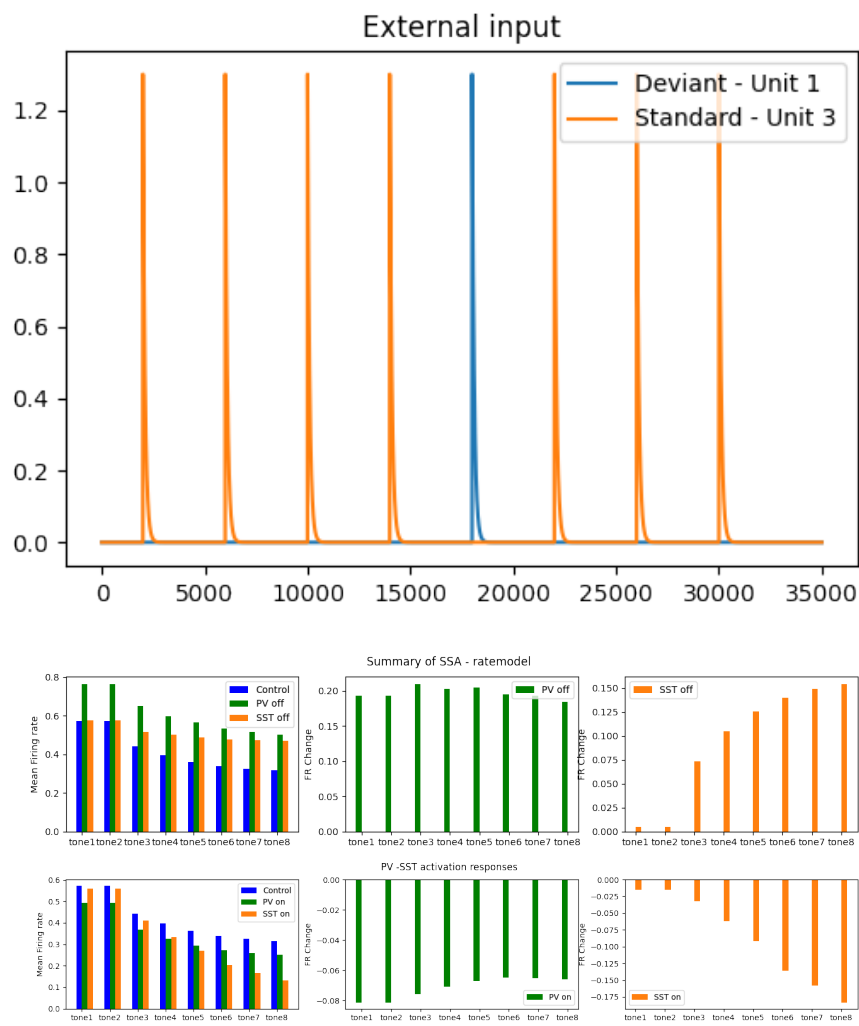


Figure 4. ReFig4

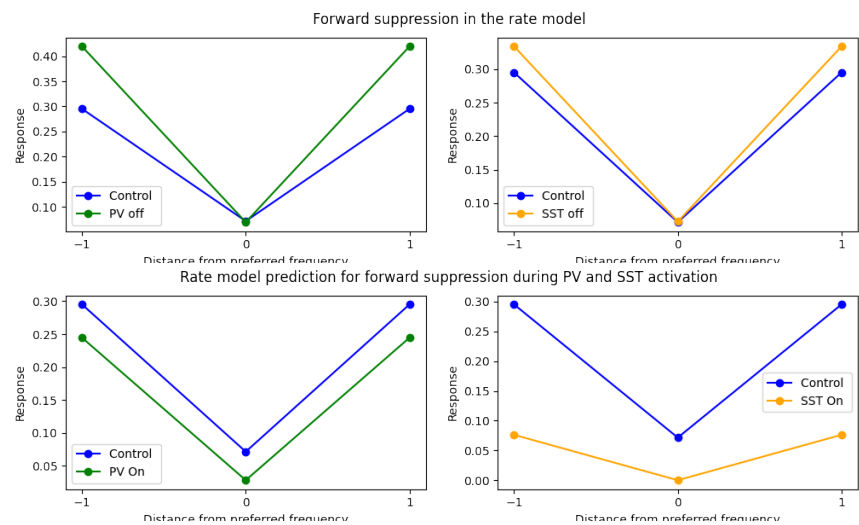


Figure 5. ReFig6

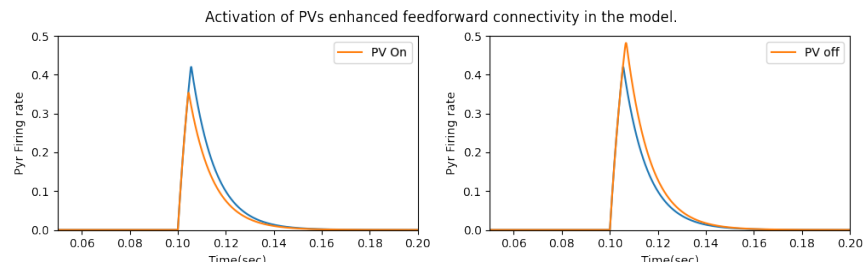


Figure 6. ReFig8

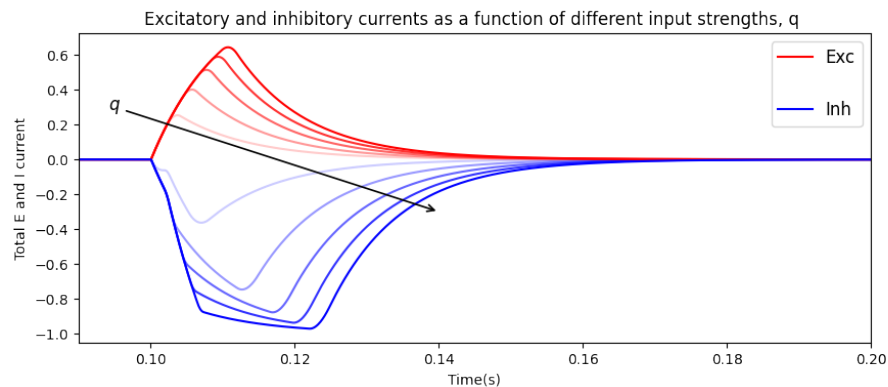


Figure 7. ReFig9

References

1. H. R. Wilson and J. D. Cowan. "Excitatory and inhibitory interactions in localized populations of model neurons." In: **Biophysical journal** 12.1 (1972), pp. 1–24.
2. M. Beierlein, J. R. Gibson, and B. W. Connors. "Two dynamically distinct inhibitory networks in layer 4 of the neocortex." In: **Journal of neurophysiology** 90.5 (2003), pp. 2987–3000.
3. M. V. Tsodyks, W. E. Skaggs, T. J. Sejnowski, and B. L. McNaughton. "Paradoxical effects of external modulation of inhibitory interneurons." In: **Journal of neuroscience** 17.11 (1997), pp. 4382–4388.
4. L. F. Abbott, J. Varela, K. Sen, and S. Nelson. "Synaptic depression and cortical gain control." In: **Science** 275.5297 (1997), pp. 221–224.
5. M. Wehr and A. M. Zador. "Synaptic mechanisms of forward suppression in rat auditory cortex." In: **Neuron** 47.3 (2005), pp. 437–445.
6. C. Cakan, C. Metzner, and N. Jajcay. **neurolib: A Python simulation framework for easy whole-brain neural mass modeling**. 2019.